1-1-2019

Large-Scale Synthesis of MOF-Derived Superporous Carbon Aerogels with Extraordinary Adsorption Capacity for Organic Solvents

Chaohai Wang

Jeonghun Kim
jhkim@uow.edu.au

Jing Tang

Jongbeom Na

Yong Kang

See next page for additional authors

Recommended Citation

Large-Scale Synthesis of MOF-Derived Superporous Carbon Aerogels with Extraordinary Adsorption Capacity for Organic Solvents

Abstract

© 2019 Wiley-VCH Verlag GmbH & Co. KGaA, Weinheim Carbon aerogels (CAs) with 3D interconnected networks hold promise for application in areas such as pollutant treatment, energy storage, and electrocatalysis. In spite of this, it remains challenging to synthesize high-performance CAs on a large scale in a simple and sustainable manner. We report an eco-friendly method for the scalable synthesis of ultralight and superporous CAs by using cheap and widely available agarose (AG) biomass as the carbon precursor. Zeolitic imidazolate framework-8 (ZIF-8) with high porosity is introduced into the AG aerogels to increase the specific surface area and enable heteroatom doping. After pyrolysis under inert atmosphere, the ZIF-8/AG-derived nitrogen-doped CAs show a highly interconnected porous mazelike structure with a low density of 24 mg cm^{-3}, a high specific surface area of 516 m2 g^{-1}, and a large pore volume of 0.58 cm^{-3} g^{-1}. The resulting CAs exhibit significant potential for application in the adsorption of organic pollutants.

Disciplines

Engineering | Physical Sciences and Mathematics

Publication Details

Authors

Chaohai Wang, Jeonghun Kim, Jing Tang, Jongbeom Na, Yong Kang, Minjun Kim, Hyunsoo Lim, Yoshio Bando, Jiansheng Li, and Yusuke Yamauchi

COMMUNICATION

A Large-Scale Synthesis of MOF-Derived Superporous Carbon Aerogels and Their Extraordinary Adsorption Capability towards Organic Solvents

Chaohai Wang+, Jeonghun Kim+, Jing Tang, Jongbeom Na, Yong-Mook Kang, Minjun Kim, Hyunsoo Lim, Yoshio Bando, Jiansheng Li* and Yusuke Yamauchi*

Abstract: *Carbon aerogels (CAs) with three dimensional (3D) interconnected networks have various promising advantages for applications such as pollutant treatment, energy storage, and electrocatalysis. Though CAs are highly desirable, it remains challenging to synthesize high-performance CAs in large scale via a simple and sustainable strategy. In this work, we provide an eco-friendly method for scalable synthesis of ultralight and superporous CAs by using cheap and widely available agarose biomass as the carbon precursor. Zeolitic imidazolate framework-8 (ZIF-8) with high porosity is introduced into the agarose (AG) aerogels to vastly increase specific surface area and enable heteroatom doping. After pyrolysis under inert atmosphere, ZIF-8/AG derived nitrogen-doped CAs show a highly interconnected porous mazelike structure, displaying a low density of 24 mg cm^{-3}, a high specific surface area of 516 m^2 g^{-1}, and a large pore volume of 0.58 cm^{-3} g^{-1}. The resulting CAs exhibit a significant potential application in the adsorption of organic pollutants. This unique strategy may inspire future exploration of new nanoarchitectures of CAs from other MOF materials with unique properties toward many industrial applications.*

C. Wang, Prof. J. Li
Jiangsu Key Laboratory of Chemical Pollution Control and Resources Reuse, Key Laboratory of New Membrane Materials, Ministry of Industry and Information Technology, School of Environmental and Biological Engineering, Nanjing University of Science and Technology, Nanjing 210094, People's Republic of China. E-mail: lijsh@njust.edu.cn
Dr. J. Kim, Prof. Y. Yamauchi
Key Laboratory of Eco-chemical Engineering, College of Chemistry and Molecular Engineering, Qingdao University of Science and Technology, Qingdao 266042, China
C. Wang, Dr. J. Kim, Dr. J. Tang, Dr. J. Na, M. Kim, H. Lim, Prof. Y. Yamauchi
School of Chemical Engineering and Australian Institute for Bioengineering and Nanotechnology (AIBN), The University of Queensland, Brisbane, Queensland 4072, Australia.
E-mail: y.yamauchi@uq.edu.au
Prof. Y. M. Kang
Department of Materials Science and Engineering, Korea University, Seoul, 02841, Republic of Korea
Prof. Y. Bando
Institute of Molecular Plus, Tianjin University, No. 92 Weijin Road, Nankai District, Tianjin, 300072 P. R. China
Prof. Y. Bando
Australian Institute of Innovative Materials (AIIM), The University of Wollongong, Squires Way, North Wollongong, NSW 2500, Australia
Prof. Y. Bando, Prof. Y. Yamauchi
International Center for Materials Nanoarchitectonics (MANA), National Institute for Materials Science (NIMS), 1-1 Namiki, Tsukuba, Ibaraki 305-0044, Japan
Prof. Y. Yamauchi
Department of Plant & Environmental New Resources, Kyung Hee University, 1732 Deogyeong-daero, Giheunggu, Yongin-si, Gyeonggi-do 446-701, South Korea

+ These authors equally contributed to this work.

materials with unique properties toward many industrial applications.

Carbon aerogels (CAs) are well-known for their physical advantages such as a large specific surface area, low density, and high porosity. Consequently, they have been widely utilized in various applications, including environmental treatment, energy storage, and chromatographic separation.[1] Over the past decades, an enormous amount of efforts have been dedicated to develop new methods to produce high-performance CAs. Conventional synthetic strategies of CAs include two steps: (i) polymerization of organic molecules into highly cross-linked gels (*e.g.*, phenol-formaldehyde), and (ii) pyrolysis of the polymerized organic aerogels under inert atmosphere.[2] For instance, Pekala *et al.* reported the resorcinol and formaldehyde as the precursors to obtain the organic aerogels, which greatly promoted the development of polymer-derived CAs.[3] However, synthesis of polymer-derived CAs is quite complex as it requires multiple polymerization processes with specific initiators for each polymerization.

Particularly, introducing sub-units into the three-dimensional (3D) CAs can allow greater control over the surface area and mechanical characteristics of CAs, thus resulting in a rapid expansion of the application of CAs.[4] Due to their impressive physical properties (*e.g.*, tensile strength, high elasticity, and low density), typical carbon nanostructures such as one-dimensional carbon nanotubes (CNTs)[5] and two-dimensional (2D) graphene[6] have been utilized for preparing new types of CAs. Although the CNT- and graphene-based CAs show enhanced conductivity and mechanical properties, which are beneficial for various applications, practical applications of them have not been realized as it is still challenging to produce them in large-scale. It is not easy to synthesize high-quality CNTs and graphene in large-scale because it requires advanced equipment and multiple chemical reactions. Therefore, it is highly desirable yet remains challenging to produce scalable high-performance CAs through simple and sustainable strategies.

Biomass polymers, which are cost-effective, abundantly available and environmental friendly, have been one of the most suitable build blocks for emerging aerogels.[7] Up to date, many biomass-based aerogels have been successfully prepared, for example, cellulose, polysaccharide, chitin, and lignin. Among them, polysaccharides are suggested to be the most suitable building blocks for aerogels due to their high abundancy in the nature.[7c] Metal-organic frameworks (MOFs), such as ZIF-8 and ZIF-67, are crystalline compounds formed *via* coordination bonding between metal ions and organic ligands. MOFs have been widely exploited as outstanding precursors for the preparation of functional carbon materials.[8] Considering the advantages of polysaccharide and MOFs, herein, we develop a facile freeze-drying and carbonization

method to prepare functionalized CAs based on biomass and MOFs precursors for the first time. Agarose (AG), one of most abundant polysaccharides in the nature, is utilized as the building blocks for aerogel. ZIF-8, well-known for its high specific surface area and nitrogen content,[9] is adopted as the sub-units and embedded into AG aerogel to form ZIF-8/AG composite aerogel. After carbonization of ZIF-8/AG, hierarchical porous CAs are obtained (denoted as ZIF-8/AG-CA). The optimized ZIF-8/AG-CA exhibits a low density (24 mg cm^{-3}), high specific surface area (516 m^2 g^{-1}), large hierarchical pore volume (0.58 cm^{-3} g^{-1}), showing outstanding performance for adsorption of various organic pollutants.

AG can be well dispersed in water upon heating at temperature above 65 °C (**Figure 1a**).[10] AG molecules can then undergo self-assembly into a robust hydrogel consisting of interconnected porous sheets after cooling down to room temperature. The synthetic steps of ZIF-8/AG-CA are shown in **Figure 1** (See more details in the *Supporting Information*). In the first step, the prepared uniform ZIF-8 nanoparticles (**Figure S1**) are dispersed in deionized water *via* sonication. Then, AG powder is added into the above solution with stirring at 65 °C for 4 hours to obtain homogeneous liquid phase (ZIF-8/AG solution, **Figure 1a**). After cooling down, the precursors are self-assembled into ZIF-8/AG hydrogels (**Figure 1b**), and the hydrogel is subsequently subjected to freeze-drying to form ZIF-8/AG aerogel (**Figure 1c**). The resulting ZIF-8/AG aerogel is finally carbonized into ZIF-8/AG-CA under N$_2$ atmosphere at 900 °C (**Figure 1d**). To investigate the influence of the loading amount of ZIF-8, three types of ZIF-8/AG-CAs with different ratios of ZIF-8 and AG are also prepared (*i.e.*, the mass ratios of ZIF/AG are 0.5, 1.0 and 2.0, denoted as ZIF-8/AG-CA-0.5, ZIF-8/AG-CA-1.0, and ZIF-8/AG-CA-2.0, respectively). It is noteworthy that scalable synthesis of ZIF-8/AG-CA has become possible with highly abundant and cost-effective AG precursors, as well as simple and efficient synthetic process (as shown in **Figure S2**). We expect industrial-scale of synthesis can be also achieved by increasing the size of reaction vessel.
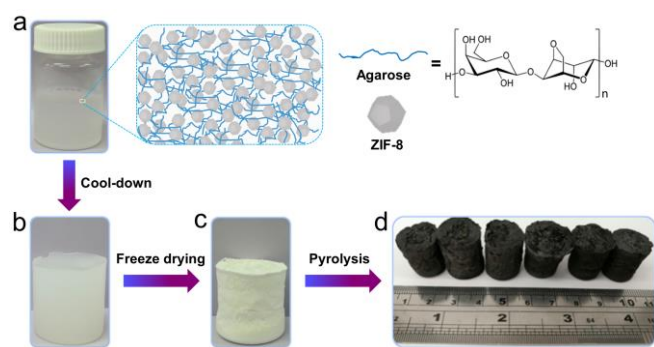

Figure 1. Preparation steps for ZIF-8/AG-CA. a) ZIF-8/AG solution, b) ZIF-8/AG hydrogel, c) ZIF-8/AG aerogel, and d) ZIF-8/AG carbon aerogel (ZIF-8/AG-CA), respectively.

As observed from scanning electron microscopy (SEM) images (**Figure S3**), the ZIF-8/AG aerogels with different ZIF/AG ratios have a 2D layer structure. The enlarged SEM images (**Figures S3b, S3d,** and **S3f**) show that ZIF-8 nanoparticles are deposited on the AG layers. The level of aggregation between ZIF-8 nanoparticles increases upon higher loading amount of ZIF-8 nanoparticles. Through direct pyrolysis, ZIF-8/AG aerogels are converted into ZIF-8/AG-CAs. The obtained ZIF-8/AG-CAs retain the shape from the original ZIF-8/AGs, although there are volume shrinkage of 67 % (for ZIF-8/AG-0.5), 42 % (for ZIF-8/AG-1.0), and 34 % (for ZIF-8/AG-2.0). The typical ZIF-8/AG-CA-1.0 has a low density of 24 mg cm^{-3},

which is highly light that it can even stand on tips of *Metrosideros Excelsa* (**Figure 2a**). **Figure 2b** shows the layered structures of ZIF-8/AG-CA-1.0 with micrometer scale lateral dimension. As shown in the magnified SEM image (**Figure 2c**), ZIF-8 nanoparticles are transformed to porous hollow structure with mazelike internal carbon framework. This is further confirmed by the TEM images (**Figure 2d** and **Figure S4a**), in which ZIF-8 derived porous hollow mazelike carbon nanoparticles are well dispersed on AG derived carbon layers. To understand the formation mechanism of such interesting hollow structures the role of AG is further investigated. In the absence of AG, ZIF-8 nanoparticles are shrunk individually and converted to typical ZIF-8 derived nanoporous carbon particles (**Figure S5**). However, in the presence of AG, the interactions between ZIF-8 and AG molecules, the AG layers provide an external force that pull the ZIF-8 "outward", thus leading to the transformation of ZIF-8 nanoparticles into a porous hollow structure upon pyrolysis at 900 °C.

The ratio of ZIF-8 to AG is important for obtaining high-quality ZIF-8/AG-CA. Homogeneously dispersed ZIF-8 derived carbon nanoparticles in ZIF-8/AG-CAs can be obtained when the mass ratio of ZIF/AG is controlled in the range from 0.5 to 2.0 (**Figure S6**). If the amount of ZIF-8 is too low, the aerogels experience a significant shrinkage during the carbonization, leading to a high density and low porosity. On the other hand, if the content of ZIF-8 is too high in ZIF-8/AG, ZIF-8 nanoparticles tend to be highly aggregated,[11] resulting in low specific surface area and fragile ZIF-8/AG-CA. Furthermore, AG alone without ZIF-8 cannot maintain its unique 2D layered structure upon pyrolysis (**Figure S7**). N$_2$ adsorption-desorption measurements were carried out to determine the specific surface areas and pore size distributions in ZIF-8/AG-CA. As shown in **Figure 2e-f**, they typical ZIF-8/AG-CA-1.0 has a large surface area of 516 m^2 g^{-1} and hierarchical porous structure with micropores and mesopores. As seen in **Figure S8a-b** and **Table S1**, the loading amount of ZIF-8 has clear effect on the distribution of pores. The ZIF-8/AG-CA-1.0 possesses the highest surface area and the largest pore volume compared to the ZIF-8/AG-CA-0.5 and ZIF-8/AG-CA-2.0.
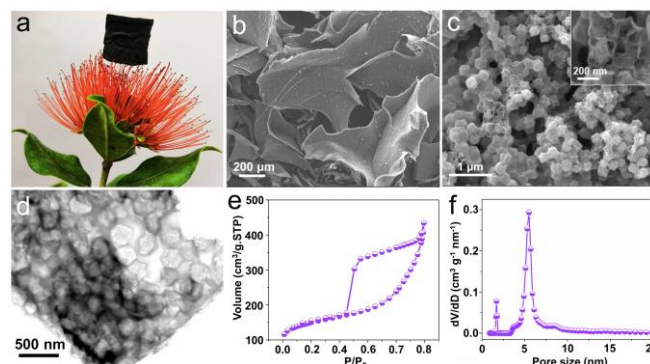

Figure 2. a) Photograph of the lightweight ZIF-8/AG-CA-1.0 standing on *Metrosideros Excelsa*. b, c) SEM and d) TEM images showing the microstructure of ZIF-8/AG-CA-1.0, (e, f) N$_2$ adsorption-desorption isotherm and pore size distribution curve of ZIF-8/AG-CA-1.0.

The composition and graphitic degree of the typical ZIF-8/AG-CA-1.0 were analyzed by X-ray photoelectron spectroscopy (XPS), X-ray powder diffraction (XRD), and Raman spectroscopy. As observed from **Figure 3a**, the XPS spectrum confirms that the ZIF-8/AG-CA-1.0 is composed of C, N, and O (**Table S1**). The high-resolution N 1s spectra (**Figure 3b**) can be deconvoluted into four peaks, pyridinic N (398.4 eV), pyrrolic N (399.5 eV), oxidized-N (401 eV), and graphitic-N (402.8 eV), respectively.[11] There is no Zn

content, indicating that it can be evaporated during carbonization process at high temperature (at 900 °C for 3 hours).[12] Furthermore, the N contents of the ZIF-8/AG-CAs increase with the increased ratio of ZIF-8, as shown in **Table S1**. Wide-angle XRD patterns of the ZIF-8/AG-CAs show the two broad diffraction peaks at around 25° and 44° (**Figure 3c** and **Figure S8c**), indicating the low degree of graphitization of carbon.[13] Raman spectra (**Figure 3d** and **Figure S8d**) show two characteristic peaks at 1350 (D) and 1580 cm^{-1} (G), revealing the coexistence of graphitic and disordered carbons. The lattice spacing of graphitic carbon can be clearly seen from the HRTEM image (**Figure S4b**). The I_D/I_G ratio are 1.12 (for ZIF-8/AG-CA-0.5), 1.17 (for ZIF-8/AG-CA-1.0), and 0.99 (for ZIF-8/AG-CA-2.0), respectively. Based on the above analysis, the addition of ZIF-8 not only plays a key role in the formation of the highly hierarchical porous structures but also influences the graphitic degree and the N content of the resulting CAs.
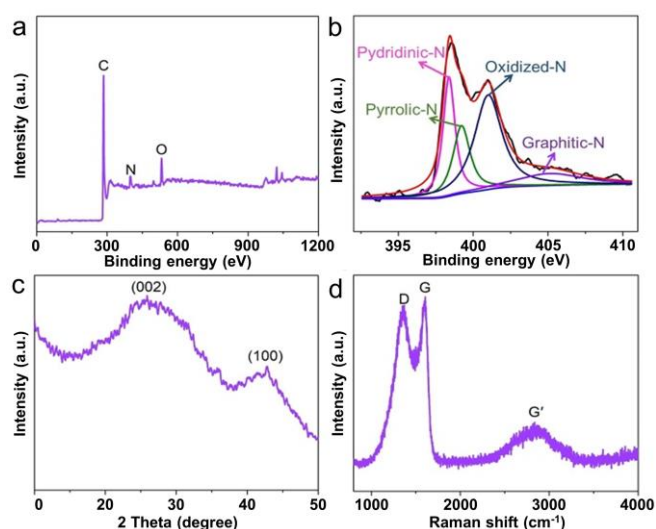

Figure 3. (a) XPS spectrum, (b) high resolution N 1s spectra, (c) wide-angle XRD pattern and (d) Raman spectrum of ZIF-8/AG-CA-1.0.

3D network porous structures with large surface area and low density are favorable for applications in many fields such as environmental remediation, energy storage and conversion, and separation.[14] As a proof-of-concept, organic solvent adsorption performance of the obtained ZIF-8/AG-CAs is evaluated. As shown in **Figure 4a**, the ZIF-8/AG-CA-1.0 can float on the water and n-hexane due to its low density. **Figure S9** shows that the ZIF-8/AG-CA-1.0 ratios exhibit the highest adsorption capacity for the typical organic solvent n-hexane and sunflower oil among all the ZIF-8/AG-CAs with different ZIF-8/AG ratios. Therefore, ZIF-8/AG-CA-1.0 was chosen as the representative adsorbent for investigating the adsorption performance of common organic solvents. As shown in **Figure 4b**, the ZIF-8/AG-CA-1.0 demonstrates an outstanding adsorption capacity for different organic solvents and common oil. It can uptake 30-60 times of its weight, which is higher than previously reported aerogels, membranes and nanomaterials, *etc*. (**Figure S10**). Commercially available graphene and CNT powders were examined for references. The n-hexane adsorption capacities of graphene and CNT are 2736 and 2785, respectively, showing lower adsorption performance than ZIF-8/AG-CA-1.0. The adsorption capacity of ZIF-8/AG-CA-1.0 shows linear relationship towards the density of corresponding organic solvent (**Figure S11**). To further evaluate the adsorption performance of our material, we also investigated five additional common solvents (**Table S2**). The

same linear relationship between the adsorption capacity and solvent density is observed for the five additional organic solvents as well, thus confirming the superior adsorption capacity of ZIF-8/AG-CA-1.0. In addition, oil/water separation was carried out to demonstrate its superior adsorption performance in practical application set-up. As shown in the **Figure S12**, the ZIF-8/AG-CA-1.0 exhibits quick adsorption of n-hexane (coloured with Sudan III) floating on water, indicating its potential application for the facile removal of oil spillage.

Due to its hierarchical porous structures, the adsorption rate of ZIF-8/AG-CA-1.0 for organic solvents is significantly high, reaching its maximum capacity in only 30 s. As an ideal adsorbent for the practical application, the reusability is crucial. Herein, we select EtOH and n-hexane as the model of polar and nonpolar solvents, respectively, for recycling tests. The adsorbed organic solvents can be easily extracted by simple heating treatment. The detailed experimental procedure is given in the supporting information. As observed from **Figure 4c-d**, even after 20 cycles, the absorption capacity remains 99.3 % for EtOH and 99.4 % for n-hexane, showing highly robust porous structure of ZIF-8/AG-CA.

In summary, we have demonstrated a simple and sustainable method for the fabrication of CAs by carbonization of ZIF-8/AG aerogels. The 3D network structures with interconnected nitrogen-doped porous structure of ZIF-8/AG-CAs are formed by the synergistic effect of ZIF-8 and AG: (*i*) ZIF-8 helps to keep the 2D layers of AG and (*ii*) AG pull ZIF-8 "outward" and convert into porous hollow structure during the carbonization. Our ZIF-8/AG-CA demonstrates an outstanding adsorption capacity towards different organic solvents and common oil. It can uptake 30-60 times of its weight, which is higher than other published data. With their inherent physical and chemical advantages, arising from highly interconnected porous structures, we expect ZIF-8/AG-CAs can be versatilely adopted to numerous environment and energy applications, such as advanced oxidation process (AOPs), supercapacitors, and rechargeable batteries. Furthermore, this sustainable strategy is easily extendable to other various types of MOF. ZIF-67 containing Co^{2+} ions can be easily prepared and dispersed in aqueous medium. Through the same experimental procedure, ZIF-67/AG aerogel with a high degree of graphitization was successfully obtained (**Figure S13**), which will be reported soon. The present work is significant for the development of CAs materials and provides new insight into the fabrication of MOF-based functional materials.
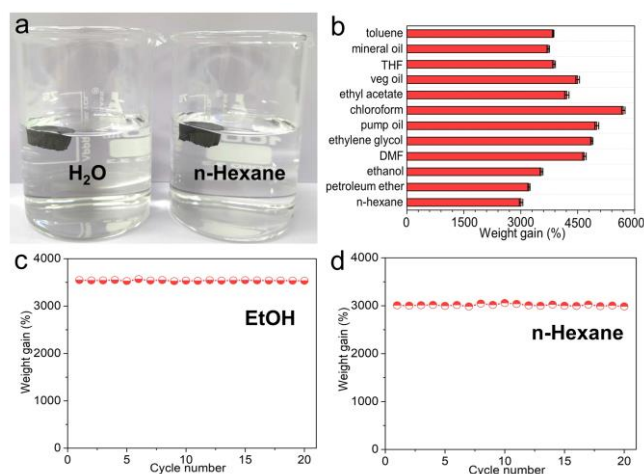

Figure 4. (a) Photographs showing the ZIF-8/AG-CA-1.0 can float on the water and n-hexane. (b) Absorption efficiency of ZIF-8/AG-CA1.0 towards commonly used organic solvents and oil. (c, d)

Recyclability tests of absorption capacities of ZIF-8/AG-CA-1.0 for EtOH and n-hexane.

Conflicts of interest

The authors have no conflicts to declare.

Keywords: carbon aerogels • metal-organic frameworks • nanoarchitectured materials • agarose • mesoporous materials

[1] a) Z. Y. Wu, H. W. Liang, B. C. Hu, S. H. Yu, *Angew. Chem. Int. Ed.* **2018**, 57, 15646; b) H. W. Liang, Q. F. Guan, L. F. Chen, Z. Zhu, W. J. Zhang, S. H. Yu, *Angew. Chem. Int. Ed.* **2012**, 51, 5101; c) F. Guo, Y. Jiang, Z. Xu, Y. Xiao, B. Fang, Y. Liu, W. Gao, P. Zhao, H. Wang, C. Gao, *Nat. Commun.* **2018**, 9, 881.

[2] S. C. Li, B. C. Hu, Y. W. Ding, H. W. Liang, C. Li, Z. Y. Yu, Z. Y. Wu, W. S. Chen, S. H. Yu, *Angew. Chem. Int. Ed.* **2018**, 57, 7085.

[3] R. W. Pekala, *J. Mater. Sci.* 1989, 24,3221.

[4] X. Gui, J. Wei, K. Wang, A. Cao, H. Zhu, Y. Jia, Q. Shu, D. Wu, *Adv. Mater.* **2010**, 22, 617.

[5] M. B. Bryning, D. E. Milkie, M. F. Islam, L. A. Hough, J. M. Kikkawa, A. G. Yodh, *Adv. Mater.* **2007**, 19, 661.

[6] a) X. Hu, W. Xu, L. Zhou, Y. Tan, Y. Wang, S. Zhu, J. Zhu, *Adv. Mater.* **2017**, 29, 1604031; b) H. Bi, X. Xie, K. Yin, Y. Zhou, S. Wan, L. He, F. Xu, F. Banhart, L. Sun, R. S. Ruoff, *Adv. Funct. Mater.* **2012**, 22, 4421; c) H. Hu, Z. Zhao, W. Wan, Y. Gogotsi, J. Qiu, *Adv. Mater.* **2013**, 25, 2219.

[7] a) T. Raj kumar, G. Gnana Kumar, A. Manthiram, *Adv. Energy Mater.* **2019**, 9, 1803238; b) X. L. Wu, T. Wen, H. L. Guo, S. Yang, X. Wang, A. W. Xu, *ACS Nano* **2013**, 7, 3589; c) J. Song, C. Chen, Z. Yang, Y. Kuang, T. Li, Y. Li, H. Huang, I. Kierzewski, B. Liu, S. He, T. Gao, S. U. Yuruker, A. Gong, B. Yang, L. Hu, *ACS Nano* **2018**, 12, 140.

[8] a) R. R. Salunkhe, Y. V. Kaneti, J. Kim, J. H. Kim, Y. Yamauchi, *Acc. Chem. Res.* **2016**, 49, 2796; b) C. Wang, C. Liu, J. Li, X. Sun, J. Shen, W. Han, L. Wang, *Chem. Commun.* **2017**, 53, 1751; c) C. Wang, Y. V. Kaneti, Y. Bando, J. Lin, C. Liu, J. Li, Y. Yamauchi, *Mater. Horiz.* **2018**, 5, 394; d) B. Liu, H. Shioyama, T. Akita, Q. Xu, *J. Am. Chem. Soc.* **2008**, 130, 5390; e) S. Dang, Q. L. Zhu, Q. Xu, *Nat. Rev. Mater.* **2017**, 3, 17075; f) P. Pachfule, D. Shinde, M. Majumder, Q. Xu, *Nat. Chem.* **2016**, 8, 718; g) C. Wang, J. Kim, J. Tang, M. Kim, H. Lim, V. Malgras, J. You, Q. Xu, J. Li, Y. Yamauchi, *Chem* **2019**, DOI: 10.1016/j.chempr.2019.09.005; h) X. Zhao, P. Pachfule, S. Li, J. R. J. Simke, J. Schmidt, A. Thomas, *Angew. Chem. Int. Ed.* **2018**, *57*, 8921.

[9] J. Tang, R. R. Salunkhe, J. Liu, N. L. Torad, M. Imura, S. Furukawa, Y. Yamauchi, *J. Am. Chem. Soc.* **2015**, 137, 1572.

[10] Q. Zhang, Y. Zhou, F. Xu, H. Lin, Y. Yan, K. Rui, C. Zhang, Q. Wang, Z. Ma, Y. Zhang, K. Huang, J. Zhu, W. Huang, *Angew. Chem. Int. Ed.* **2018**, 57, 16436.

[11] C. Liu, J. Wang, J. Li, J. Liu, C. Wang, X. Sun, J. Shen, W. Han, L. Wang, *J. Mater. Chem. A* **2017**, 5, 1211.

[12] a) C. Wang, J. Kim, M. Kim, H. Lim, M. Zhang, J. You, J. H. Yun, Y. Bando, J. Li, Y. Yamauchi, *J. Mater. Chem. A* **2019**, 7, 13743; b) Y. Pan, K. Sun, S. Liu, X. Cao, K. Wu, W. Cheong, Z. Chen, Y. Wang, Y. Li, Y. Liu, D. Wang, Q. Peng, C. Chen, and Y. Li, *J. Am. Chem. Soc*. **2018**, 140, 7, 2610; c) P. Yin, T. Yao, Y. Wu, L. Zheng, Y. Lin, W. Liu, H. Ju, J. Zhu, X. Hong, Z. Deng, G. Zhou, S. Wei, and Y. Li, *Angew. Chem. Int. Ed*. **2016**, 55, 10800.

[13] W. Xia, J. Tang, J. Li, S. Zhang, K. C. Wu, J. He, Y. Yamauchi, *Angew. Chem. Int. Ed.* **2019**, DOI: 10.1002/anie.201906870.

[14] a) J. D. Yi, M. D. Zhang, Y. Hou, Y. B. Huang, R. Cao, *Chem. Asian J.* **2019**, DOI: 10.1002/asia.201900727; b) T. Shang, Z. Lin, C. Qi, X. Liu, P. Li, Y. Tao, Z. Wu, D. Li, P. Simon, Q. H. Yang, *Adv. Funct. Mater.* **2019**, 29, 1903960; c) H. Ou, P. Yang, L. Lin, M. Anpo, X. Wang, *Angew. Chem. Int. Ed.* **2017**, 56, 10905; d) Z. L. Yu, G. C. Li, N. Fechler, N. Yang, Z. Y. Ma, X. Wang, M. Antonietti, S. H. Yu, *Angew. Chem. Int. Ed.* **2016**, 55, 14623.

COMMUNICATION

C. Wang, J. Kim, J. Tang, J. Na, Y. M. Kang, M. Kim, H. Lim, Y. Bando, J. Li* and Y. Yamauchi*

A Large-Scale Synthesis of MOF-Derived Superporous Carbon Aerogels and Their Extraordinary Adsorption Capability towards Organic Solvents
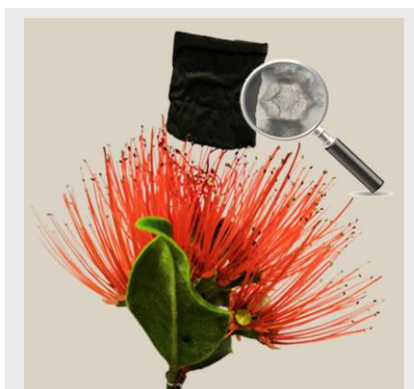
MOF-based carbon aerogels (CAs) have been fabricated *via* a simple and sustainable strategy in large scale. The obtained CAs show highly interconnected porous structure, displaying a low density of 24 mg cm^{-3}, a high specific surface area of 516 m^2 g^{-1}, and a large pore volume of 0.58 cm^{-3} g^{-1}. The resulting CAs shows a significant potential application in the adsorption of organic pollutants.